28/IV-84

2/27/84

E4-84-67

R.A.Eramzhyan[1], M.Gmitro, T.D.Kaipov[2], S.S.Kamalov, R.Mach

PION PHOTOPRODUCTION AND RADIATIVE PION CAPTURE ON NUCLEI

[1]Institute for Nuclear Research, Moscow, USSR, 117312
[2]Kazakh State University, 480-091, Alma-Ata, USSR

1984

1. INTRODUCTION*

Extensive programmes of investigations of nuclear transitions to the discrete states of residual nuclei have been initiated during the last years in several laboratories. A wide variety of reactions is used for this purpose: nucleon and pion scattering and charge-exchange, in-flight and at-rest radiative pion capture, pion photoproduction, etc.

Traditionally the interactions of elementary particles with atomic nuclei are considered within the multiple-scattering scheme. The nucleons are assumed to be the only nuclear constituents, and then equations are derived, which connect the projectile-nucleus amplitude with the elementary projectile-nucleon process and the nuclear transition densities. Recently, it has also been suggested, that the non-nucleonic degrees of freedom should be included explicitly in such calculations. Specifically, the interaction of Δ resonance propagating through the nucleus has been frequently considered, e.g., within the so-called resonance-hole $(N^{-1}\Delta)$ model. In our opinion at the present stage of investigations one should check the simplifying assumptions introduced when solving the equations and develop a consistent scheme for a unified description of the possibly broader range of different types of reactions. Such a global problem subdivides naturally into several points: (i) the construction of the amplitude for an elementary process, (ii) the description of the particle propagation through the nuclear medium, and (iii) the construction of the model nuclear states involved in the transition.

One may judge about the reliability of conceptions used comparing the calculated characteristics with experimental data. Unfortunately, the complex nature of the calculations just mentioned makes such an analysis very difficult. One cannot vary simultaneously all the input information, and the final results depend therefore strongly on the reliability of the assuptions which have been taken for granted. Along this line, one avoids a great deal of difficulties using, e.g., the nuclear structure information extracted from a relatively simple and well studied process. In practice it is usually the e^- scattering which can suit this purpose.

In the present report we discuss mainly the charged pion photoproduction and radiative pion capture on 1p -shell nuclei, taking as examples ^{10}B, ^{12}C, and ^{16}O and using the electron-

---

*Invited talk at Workshop on Perspectives in Nuclear Physics at Intermediate Energies. Trieste, 10-14 October, 1983.

and pion-scattering data for the consistency checks. As to the pion photoproduction in the few-body systems, the problem was discussed in a systematic way in refs. [1,2]. Three nuclei were selected here since we possess a variety of experimental data for them. The partial transitions in $1p$ -shell nuclei were the subject of discussion already in refs. [3,4]. We will not repeat the known results and rather discuss the new aspects seen in more recent investigations.

2. ELEMENTS OF PION PHOTOPRODUCTION THEORY

Theory of pion photoproduction on complex nuclei is given in refs. [1,3]. It is based on the distorted wave impulse approximation (DWIA). The mesonic exchange currents - the development of which goes beyond IA - were considered in the few body systems [2]. The distortion of pionic waves is taken into account usually through the pion-nucleus optical potential. For the problems to be discussed in this report it is more convenient to start with the Lippmann-Schwinger equation for the pion-nucleus system. This representation was used already in ref. [5] for the pion scattering problem, and in ref. [6] for the pion photoproduction.

2.1. Following ref. [6] the partial transition amplitude for pion photoproduction on complex nuclei in the total-momentum, j, representation reads,

$$F_{no}^{\gamma j}(\pi,\gamma) = V_{no}^{\gamma j}(\pi,\gamma) - \frac{1}{\pi}\sum_{n'\pi'}\int \frac{q'\,dq'\,F_{nn'}^{j}(\pi,\pi')\,V_{n'o}^{\gamma j}(\pi',\gamma)}{M_{n'}(q')[E_h(q)-E_{n'}(q')+i\epsilon]}. \quad (1)$$

The amplitude (1) describes the absorption of a photon with quantum numbers $|\gamma\rangle = |J_\gamma, k\lambda\rangle$ and creation of a pion with quantum numbers $|\pi\rangle = |L_\pi, q\rangle$ connected with the nuclear transition from the ground $|0\rangle$ to an excited state $|n\rangle$. The first term in (1)

$$V_{no}^{\gamma j}(\pi,\gamma) = \langle L_\pi q; J_n | V^{\gamma j} | J_\gamma k\lambda; J_o\rangle \quad (2)$$

is the plane-wave part of the partial amplitude. The pion-nucleus interaction enters into the amplitude $F_{no}^{\gamma j}(\pi,\gamma)$ through the second term of expression (1), where $E_n(q) = E_\pi(q) + E_A^n(q)$ is the total energy of the system. One can find the partial amplitude for pion-nuclear scattering $F_{nn'}^{j}(\pi,\pi')$ solving the system of Lippmann-Schwinger equations:

$$F_{nn'}^{j}(\pi,\pi') = V_{nn'}^{j}(\pi,\pi') - \frac{1}{\pi}\sum_{n''\pi''}\int \frac{\bar{q}^2\,d\bar{q}}{M_{n''}(\bar{q})} \frac{V_{nn''}^{j}(\pi,\pi'')\,F_{n''n'}^{j}(\pi'',\pi')}{[E_n(q)-E_{n'}(\bar{q})+i\epsilon]} \quad (3)$$

The first term - $V_{nn'}^{j}(\pi,\pi')$ - is again the plane-wave part of the scattering amplitude. The second term corresponds to the elastic and inelastic virtual rescattering and charge-exchange processes.

2.2. Now we shall list the main approximations usually invoked to solve eq.(2):
  i) $F_{nn'}(\pi,\pi') = 0$, when $n \neq n'$ and $L \neq L_\pi'$ - the coherence approximation,
  ii) $F_{nn}(\pi,\pi) = F_{oo}(\pi,\pi)$.
These assumptions constitute the basis of the DWIA method.
Next we shall single out from (3) the part connected only with the on-shell elementary amplitude. For that purpose let us represent the Green function as

$$[E_n(q)-E_{n'}(q')+i\epsilon]^{-1} = P/[E_n(q)-E_{n'}(q')]-i\pi\delta(E_n-E_{n'}). \quad (4)$$

The calculation of the pion-nucleus amplitude with the second term of the Green function (4) requires the on-shell elements only of the pion-nucleon amplitude. In this approximation and with the above assumptions one has

$$F_{no}^{\gamma j}(\pi,\gamma) = V_{no}^{\gamma j}(\pi,\gamma)[1+iqF_{oo}^{j}(\pi,\pi)]. \quad (5)$$

When the first term of the Green function is also taken into account for calculating the pion-nucleus amplitude one has to know the off-shell behaviour of the pion-nucleon amplitude.

As follows from various calculations [7] the pion-nucleus scattering is frequently described well enough when neglecting off-shell effects. Figures 1 and 2 illustrate the situation*). There we have calculated the transitions to $J^\pi T = 1^+1$, $E^* = 15.1$ MeV and $J^\pi T = 2^+1$, $E^* = 16.1$ MeV levels in ^{12}C. The reason of the substantial discrepancy at $T_\pi = 100$ MeV for the 2^+1 level is unclear yet. The same discrepancy has been observed in the much more ambitious isobar-hole model [8] as well.

One reason why the approximate method, where off-shell effects are neglected, works so well, could be the following. In the exact multiple scattering theory one may expect a cancellation of the pion-nuclear off-shell effects with the corrections to the impulse and coherence approximation. The second reason: in most of calculations the off- shell extrapolation

---

*) In talk were shown the experimental points from ref. [8]. Erroneously we used the results, which do not include the normalization factor $\sqrt{(2J_n+1)(2T_n+1)}$ when CO-form factor of the ^{12}C excited states are substituted by the ground state CO-form factor.
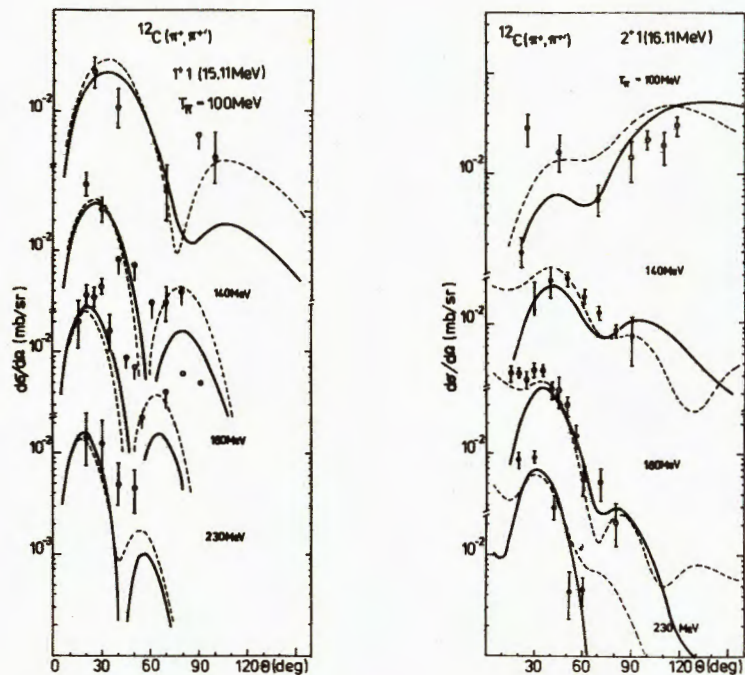
Fig.1. Differential cross section for ^{12}C$(\pi^+,\pi^{+\prime})$ ^{12}C$(1^+, 2^+; T=1)$ reaction: solid line – without off-shell extrapolation of amplitude, dashed line – with extrapolation. The experimental points are from Peterson et al. [27]. (T_π = 100, 140, 180, 230 MeV).
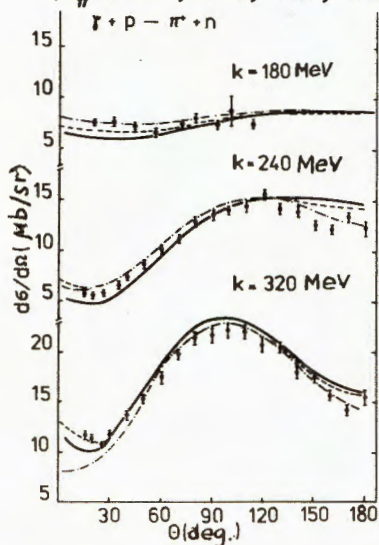

Fig.2. Differential cross section for $\gamma p \to \pi^+ n$ reaction calculated with the CGLN [9] (solid line), BL [11] (dashed line) and BDW [10] amplitudes.

is performed by the parametrization valid only in the $\Delta(33)$ region. Beyond this region the off-shell behaviour of the elementary πN amplitude is indeed an open problem.

2.3. In the impulse approximation $V^{\gamma j}_{no}(\pi,\gamma)$ is expressed in terms of $f^\lambda_{\pi\gamma}$, the amplitude of pion photoproduction on a free proton:

$$f^\lambda_{\pi\gamma} = if_1\,\vec\sigma\cdot\vec\epsilon_\lambda + f_2\,[\hat{\vec q}\times\hat{\vec k}]\cdot\vec\epsilon_\lambda + if_3\,\vec\sigma\cdot\hat{\vec k}\,\hat{\vec q}\cdot\vec\epsilon_\lambda + if_4\,\vec\sigma\cdot\hat{\vec q}\,\hat{\vec q}\cdot\vec\epsilon_\lambda. \qquad (6)$$

In (6) f_α ($\alpha = 1 \div 4$) are scalar functions. They depend on $\vec k, \vec q$ and the nucleon momentum. There are three popular versions of the amplitude $f^\lambda_{\pi\gamma}$ – CGLN [9], BDW [10] and BL [11]. The first two are derived from the dispersion relations, the last one from the phenomenological Lagrangian. All three amplitudes describe well enough the experimental data on the free proton(see Fig.2). The best agreement with experiments takes place around the angle $\theta = 90°$, where the deviations do not exceed 5%. At the same time the individual f_α in each of three versions are different in magnitude (table 1). An especially large difference is for f_2, the spin-independent part of the amplitude. For example, at $k = 260$ MeV and $\theta = 90°$ it amounts to 40%. Such a difference in f_2 does not influence the cross section on the free proton due to an overall compensation. In nuclear transitions, however, the individual f_α contribute with different weights and the compensation can be destroyed.

2.4. Now we single out the nuclear matrix elements in the amplitude $V^{\gamma j}_{no}(\pi,\gamma)$.

$$V^{\gamma j}_{no}(\pi,\gamma) = \sum_{\alpha JL}\int_{-1}^{1} dx\, C^{j\alpha JL}_{no}(\pi,\gamma;x)\,f_\alpha\,<J_n\,||\,\hat O_{LJ}(a_\alpha)\,||\,J_o>. \qquad (7)$$

In (7) C_{no} is a geometrical factor [6], $\hat O_{LJ}(a) = J_L(Qr)[Y_L \oplus a_\alpha]_J$ is a transition operator, Q – the momentum transfer to the nucleus; a_α stands for either 1 or $\vec\sigma$. For 1p-shell nuclei both the shell model [13] and the phenomenological Helm model [14] have been used to calculate the nuclear matrix elements. The electron scattering data are decisive to judge how well the matrix elements are calculated. Indeed, two types of matrix elements – spin-dependent and spin-independent – enter into the calculation of the transversal form factors. In different reactions they do not contribute in the same way. One should therefore know their magnitudes separately. Unfortunately, the (e,e′) data cannot provide such an information. Another difficulty comes from the meson exchange currents. Their nature and contribution depend again on the type of reaction studied.

Table 1

The amplitudes f_α at $\theta = 90°$ in the lab.system

k, MeV		200		260		320	
$f_\alpha \cdot 10^3$ (fm)		Re	Im	Re	Im	Re	Im
f_1	CGLN	38.1	0.2	37.5	2.1	33.6	7.0
	BDW	38.7	1.5	36.8	2.1	32.5	6.7
	BL	38.0	0.2	37.3	1.7	37.7	6.3
$-f_2$	CGLN	14.4	1.5	29.6	14.7	18.3	46.2
	BDW	18.4	1.8	33.5	15.8	21.7	47.1
	BL	20.4	1.2	37.4	12.1	29.5	41.7
f_3	CGLN	25.0	0.7	35.8	7.3	29.8	23.1
	BDW	25.4	1.3	33.9	9.8	23.1	25.4
	BL	24.4	0.6	33.2	6.0	27.6	20.9
$-f_4$	CGLN	13.5	0.0	19.6	0.0	21.9	0.0
	BDW	13.3	0.0	18.7	0.1	19.9	0.2
	BL	13.5	0.0	19.4	0.0	21.5	0.0
$d\sigma/d\Omega$ (μb/sr)	CGLN	9.44		16.47		21.24	
	BDW	9.99		16.47		20.50	
	BL	9.72		17.16		20.84	

For the 1p-shell nuclei the wave functions are frequently constructed so that only 1p-nucleons are active. The admixture of higher (2ℏω, etc.) configurations which should provide an appropriate contribution of high-momentum components to the wave functions is, however, desirable for the calculation of the form factors at a large momentum transfer and of the exchange currents. As yet, however, there is no really consistent calculation of the higher configuration effects in ^{12}C.

Let us mention some difficulties encountered in the actual analysis of electron scattering data of the 1p-shell nuclei. First of all only in a few cases there exist experimental data in a wide region of the momentum transfer. Moreover, in many cases the nuclear models do not reproduce even the existing experimental data. At the same time without solving the problem of nuclear structure input it is indeed meaningless to analyse the pionic reactions we consider here. We shall discuss now the situation in more detail.

3. THE NUCLEAR FORM FACTORS IN INELASTIC ELECTRON SCATTERING ON 1p-SHELL NUCLEI

3.1. Let us start with nuclear isovector transitions of the magnetic type. The excitation of $J^\pi T = 1^+1$, $E^* = 15.1$ MeV level in ^{12}C is an example of M1-transition. The shell model in a standard version - for example, that of Cohen and Kurath (CK)[13] roughly reproduces the M1 form factor at a low momentum transfer. In a region of the second maximum it fails, however, to reproduce the experimental data. The deficiency in this region is usually attributed to the meson-exchange-current contribution. On the other hand, a parametrization of the 1p-shell M1 transition density has been suggested (DH)[15] that describes correctly the region of the second maximum without inclusion of mesonic exchange currents. The problem is vividly discussed now, since the M1 form factors being measured very precisely in a number of nuclei are used for testing[16] the nonnucleonic degrees of freedom in the light nuclei (Δ-resonances, mesonic currents).

A good example of M2-transition exists in ^{16}O: the $J^\pi T = 2^-1$ level at 12 MeV. The shell model does not describe the electromagnetic form factor for this level satisfactorily. One can, however, fit the parameters of the wave function in a phenomenological way so as to reproduce the experimental data[17].

To show an example of the M3-transition, one can consider the excitation of $J^\pi T = 0^+1$ and the 2_1^+1 levels in ^{10}B. In the shell model both M3 form factors are well reproduced[18]. At the same time the strong M1-transition in ^{10}B associated with the 2_2^+1 level is reproduced only qualitatively in the shell model. The Helm model being a fit describes indeed this form factor well.

3.2. Let us discuss now the nuclear transitions of the electric type. Two expressions for the corresponding transition operator are:

$$T(EJ) = \frac{r_3}{2M}\left(Q\frac{\mu_p - \mu_n}{2}\hat{O}_{JJ}(\vec{\sigma})\right)\begin{cases} +[\sqrt{\frac{J+1}{2J+1}}\hat{O}_{J-1J}(\vec{\nabla}) - \sqrt{\frac{J}{2J+1}}\hat{O}_{J+1J}(\vec{\nabla})] & (8a) \\ -\sqrt{\frac{J+1}{-J}}\frac{M}{Q}(E_a - E_o)\hat{O}_{JJ}(1) - \sqrt{\frac{2J+1}{J}}\hat{O}_{J+1J}(\vec{\nabla}) & (8b) \end{cases}$$

The first expression (8a) is a standard one, the second (8b) is obtained[19,20] using the continuity equation for the nuclear

electromagnetic current. An interesting effect has been observed for E2-transitions. With the harmonic-oscillator single-particle radial function one gets the relation $(J = 2)$:

$$< 1p_j \parallel \sqrt{\tfrac{3}{5}}\, \hat{O}_{12}(\vec{\nabla}) - \sqrt{\tfrac{2}{5}}\, \hat{O}_{32}(\vec{\nabla}) \parallel 1p_{j'} > = 0. \qquad (9)$$

It is clear from (8a) that the convection-current contribution to the E2-operator vanishes identically if the nucleons occupy 1p -shell only. When the continuity equation is taken into account, a different expression follows for the convective part of the current. As a result, one avoids the accidental cancellation (9). The numerical results corresponding to eqs. (8a) and (8b) might be dramatically different.

The reason for the difference is that we use the nuclear many-body Hamiltonian H_A in the current continuity equation

$$< \vec{\nabla} \cdot \hat{\vec{j}}(\vec{r}) >_{no} = -i < [\hat{H}_A, \hat{\rho}(\vec{r})] >_{no}.$$

The excitation energy $(E_n - E_o)$ is taken therefore correctly into account. On the other hand when eq. (8a) is applied (with the one-body operators), it is equivalent to using eq. (8b), with zero effective value of $(E_n - E_o)$.

When the momentum transfer increases, the spin-dependent part of the operator becomes more important. The first term in the brackets in eq. (8b) is proportional to the operator of Coulomb excitation. At the low momentum transfer this term dominates. Its contribution is significant when the matrix element of Coulomb operator and the energy difference $(E_n - E_o)$ are large. Inspecting the nuclear wave functions one can expect the large effect from the continuity-equation constraint in the following pure E2 -transitions: in ^{12}C to the levels 2+1, $E^* = 16.1$ MeV and 2^+0, in ^7Li, ^9Be, and ^{11}B to the levels $7/2^-$ with isospin $T = 1/2$ and $3/2$, in ^{13}C - to $5/2^-$ level $(T = 1/2$ and $3/2)$. When E2 is mixed with M1 excitation, the E2 contribution into the full form factor will be changed appreciably at the low momentum transfer after exploiting the continuity equation. Examples could be the following: in ^{14}N $J^\pi T = 2^+1$ levels, in $^{13}C - 3/2^-$ levels $(T = 1/2$ and $3/2)$. In ^6Li for transitions to 2^+1 level the effect will be negligible because the C2 transition is strongly hindered. At the same time a large difference between (8a) and (8b) should be expected for the transition to 3^+0 level. Moreover in isoscalar transitions the spin-dependent term is small, therefore the relative change may be very big in that case.

3.3. Now we shall discuss quantitatively the form factor of E2-transition taking the 2^+1, $E^* = 16.1$ MeV level in ^{12}C as an example [20]. When the CK wave function is used for the calculation, the longitudinal form factor F_L^2 in the region of $Q = 0.2$-

0.5 fm^{-1} is twice overestimated (fig.3, curve 1). This is due to the limitation of the configuration space used. With $2\hbar\omega$ configurations added to the basis [21], the form factor approaches its correct value. One may neglect the $2\hbar\omega$ configurations and instead of it try to introduce an approximate scaling factors. With $\beta^2 = 0.45$ the data are reproduced [20] well (curve 2 in fig.3). In the same region of Q the CK wave function gives a lower value for the transversal form factor F_T^2 as compared with the experimental data (curve 1 at the bottom). When the continuity equation is taken into account, one gets a correct value of $F_T^2(Q)$ with the CK function using the scaling factor (curve 4) already found from F_L^2 not only at low but also at large momentum transfer - (fig.3).

In ^{12}C there are accurate data both for the longitudinal and transverse transitions to the 16.1 MeV level. It is indeed rather a rare exception. Quite different though interesting are isovector transitions to the negative-parity states at $E^* = 12$ MeV in ^{16}O. For this region of nuclear excitation a reasonably detailed experimental information on form factors exists only for 2^- level. Further the form factors are measured for the unresolved group of 0^-, 1^-, 2^- and 3^- levels, and for 3^- level, but at $\theta = 135°$ and for low values of the momentum
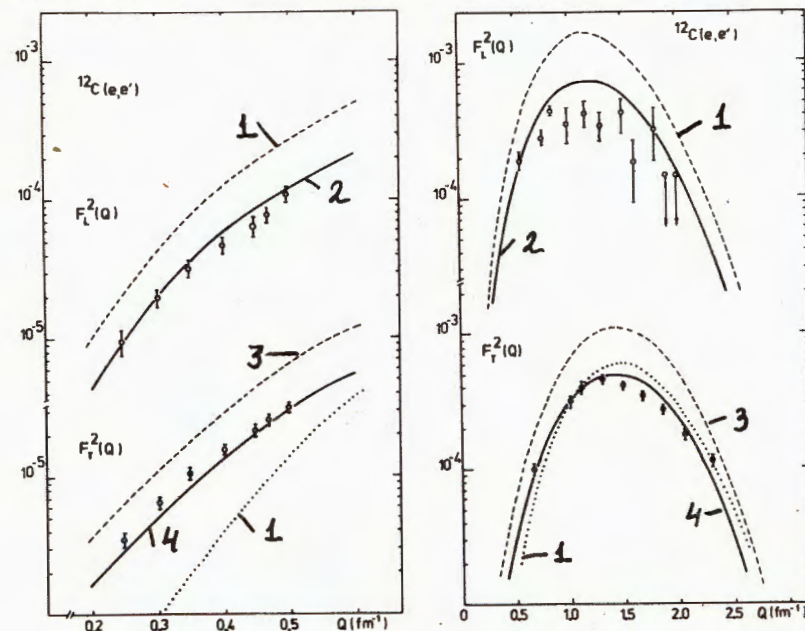

Fig.3. Electromagnetic form factors for transition to $J^\pi T = 2^+1$ level in ^{12}C. CK wave functions: 1 and 3 - without, 2 and 4 - with scaling factor. The continuity equation is used in curves 3 and 4.

transfer [14]. For 3^- level such information does not allow the determination of the matrix elements in a unique way [22] (fig.4). Indeed, both the Helm model [14] (the dashed line) and the shell model [17] (the solid line) about equally well reproduce the experimental data for the total form factor $F^2 = (\frac{1}{2} + tg^2\frac{\theta}{2})^{-1} F_L^2 + F_T^2$. However, being taken separately F_L^2 and F_T^2 differ significantly in both the models. Such a difference will influence strongly the pion photoproduction cross section. As to the continuity equation it changes indeed the calculated E1 and E3 form factors in ^{16}O as well. The present day experimental data do not, however, discriminate the calculations with and without the continuity-equation constraint.

It seems preferable to use the microscopic models to calculate the nuclear matrix elements (even if one needs to scale them afterwards) as compared with pure phenomenological analyses. The wave functions give always information on the relationship between spin-dependent and spin-independent matrix elements. Otherwise such important information is lost.

4. PHOTOPRODUCTION OF CHARGED PIONS FROM ^{10}B, ^{12}C AND ^{16}O.

4.1. The experimental data and results of the calculations are compared in figs.5 and 6 for pion photoproduction on ^{10}B at $\theta = 45°$ and $90°$. For $\theta = 90°$ the on-shell version of DWIA (solid lines) reproduces successfully the experimental data near the $\Delta(33)$ resonance energy. At lower energies the experimental data lie below calculation. The reason for that is yet unknown. The situation is not improved when the usual version of DWIA with the pion-nucleus optical potential is used [23] (dashed lines in figs. 5 and 6).

At $\theta = 45°$ the results of several calculations differ significantly [3,23]. The on-shell version of DWIA is close to the results of ref. [3]. The calculations differ most strongly in the energy region $k < 250$ MeV, where there are no experimental data.

4.2. For ^{12}C we possess data for the region $k = 180-200$ MeV only. When interpreting them a number of questions arises. The first: it is not clear why the cross section for the 1^+ level in the forward direction has always been overestimated. The second: for the 2^+ level the strong deviations are observed between the results based on the shell model (CK wave functions) and on the Helm parametrization despite the fact that both the models have predicted the E2 form factor equally well.

The on-shell DWIA calculation (fig.7) provides results in agreement with experimental data up to $\theta \approx 90°$ including the small angles [24]. Both versions of the shell-model wave functions - CK (dash-dotted line) and DH (solid line) - give practically the same value for the cross section. As to the optical
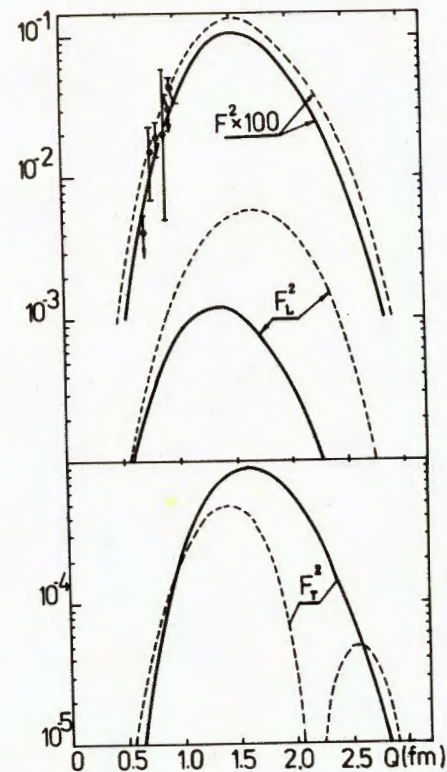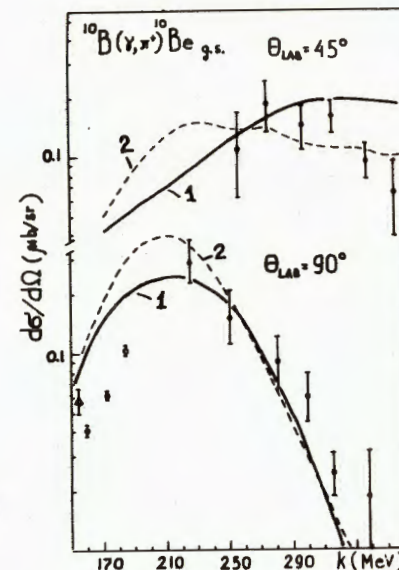

Fig.4. Electromagnetic form factor for transition to the lowest $J^\pi T = 3^-1$ level in ^{16}O. The dashed line - calculation in the Helm model, the solid line - with the DW wave function [22].

Fig.5. $d\sigma/d\Omega$ for $^{12}B(\gamma,\pi^+)$ $^{10}Be(0^+, 2_1^+)$: 1 - on-shell version of DWIA, CGLN amplitude, 2 - ref. [23].

potential version of DWIA [3], the deviation of its prediction from our on-shell calculation seems to originate from the off-shell behaviour of the amplitude. Indeed, if the second term of the Green function in eq. (4) is taken into account, then instead of the solid line one gets the result given by the dashed line in fig.7. The latter is close to the optical model version of DWIA (dotted line) [3]. In the on-shell version of DWIA it is impossible to reproduce the experimental data at $\theta > 90°$. It seems to be important for this region to take correctly into account the off-shell effects. The same situation has been observed for pion scattering in fig.1.

Now let us turn to the 2^+ level in ^{12}C. In ref. [3] (the result is shown in fig.8 by the dotted line) the CK wave function has been used without scaling. In the Helm model the continuity equation is taken into account in the long wavelength limit (i.e., without the last term in eq. (8b)). The corresponding
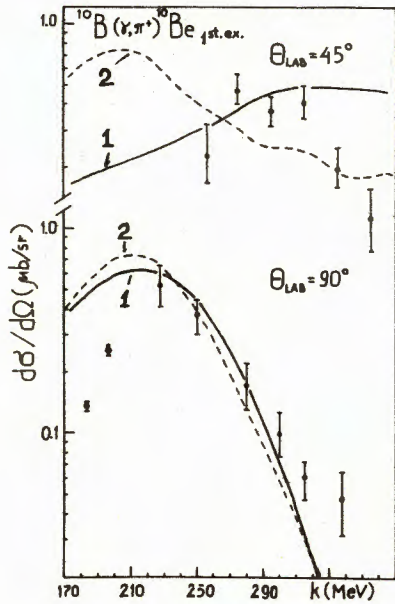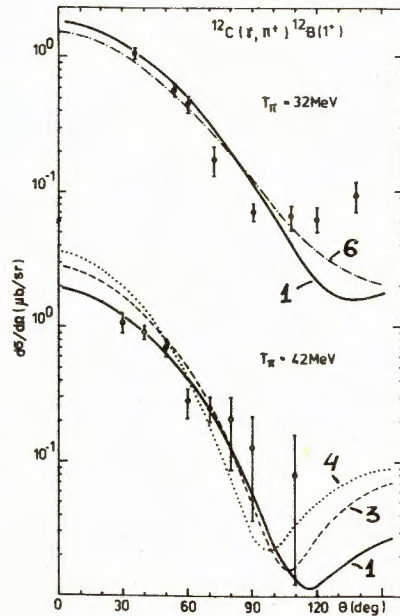
Fig.6. The same as in fig.5.

Fig.7. $d\sigma/d\Omega$ for $^{12}C(\gamma,\pi^+)$ reaction. On-shell calculations: 1 – DH, 2 – CK (scaled by $\beta^2 = 0.45$ for 2^+); 3 – off-shell effects included, DH; 4 – ref.[3], 5 – ref.[14], 6 – CK[24]
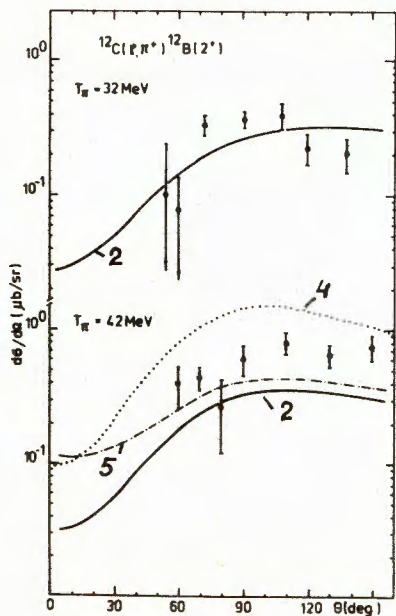
result is shown in fig.8 by the dash-dotted line. The on-shell version of DWIA with the CK function and scaling factor gives the result shown in fig.8 by the solid line. The discrepancy with data seems to be removed.

4.3. A similar problem was observed in calculations of the radiative pion capture from mesoatomic orbits. The yield R of γ-quanta when the 1^+ level of ^{12}B is populated agrees well with the experimental data. When the 2^+ state is populated, the

Fig.8. The same as in fig. 7.

yield obtained with the CK wave function without scaling is twice the experimental value [25]. Taking into account the scaling factor from the (e,e') analysis the yield becomes equal to $R(2^+)=1,57\cdot10^{-4}$. This is close to the experimental value $R = (1.29+0.25)\cdot10^{-4}$.

4.4. The energy dependence of the pion angular distribution when bound states of ^{16}N are populated is shown in fig.9 for $\theta = 45°$ and $90°$. At $\theta = 90°$ for the energy region of the $\Delta(33)$ resonance the on-shell version of DWIA with the DW [17] wave function (solid line) reproduces the experimental data. The same holds for the optical-model version of DWIA[23] (dashed line).

At $\theta = 45°$ the situation becomes very close to that observed for ^{10}B (figs.5 and 6). At $k = 220$ MeV the experimental data are located above the theoretical calculations. However at $k \approx 180$ MeV – fig.10 – the agreement is close, one should say, much too close.

The ambiguity in nuclear matrix elements (discussed in section 3.3) results in a different behaviour of the photopion cross-section. In fig.9 the results given by the shell model
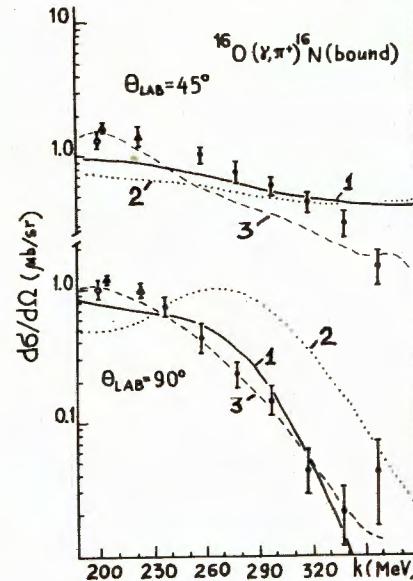
Fig.9. Differential cross section of pion photoproduction with ^{16}N in the bound states. The on-shell version of DWIA, CGLN amplitude: 1 – the DW wave function, 2 – the Helm model; 3 – the result of ref.[23].
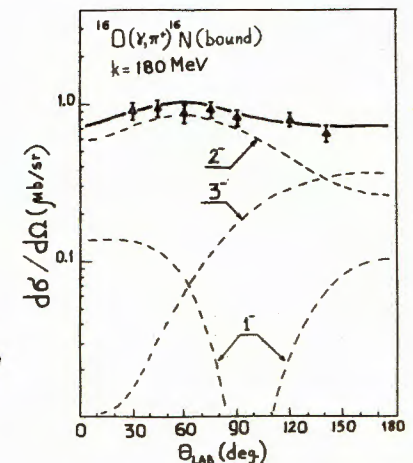
Fig.10. Photoproduction of pions in ^{16}O with ^{16}N in the bound states. The on-shell version of DWIA, DW wave function, CGLN amplitude. Experimental data from ref.[26].

and the Helm model are compared. The difference between two calculations is indeed very large. It seems that the shell model fits better the experiment.

4.5. In fig.11 two results are shown for ^{12}B populated in its ground state. One is obtained with the CK wave function (the dotted line), the other with the DH wave function (the solid line). In the first case the electromagnetic M1 form factor was reproduced after including the exchange currents only. In the second no exchange currents are required. The energy dependence of the cross section at $\theta = 90°$ and large photon energies appears to be very different. In the absence of the experimental data it is impossible to discriminate between these two versions of wave functions.

4.6. The f_2 part of the elementary amplitude (6) does not contribute to $J^\pi = 0^+ \to 1^+$, 2^-, etc., nuclear transitions in pion photoproduction. Therefore at low energies all three versions of the amplitude - CGLN, BDW, and BL - give practically the same result. When the photon energy increases, the three cross sections deviate from each other. This is due to the difference in both spin-dependent and spin-independent parts of the elementary amplitude. There is no compensation now. In nuclear $J^\pi = 0^+ \to 1^-$, 2^+, etc., transitions the difference in amplitudes manifests itself already at low energies. These transitions are

Table 2

The differential cross sections in nb/sr at $\theta = 90°$.

k, MeV		200	260	320
$^{12}B, 1^+$	CGLN	57.4	21.4	2.0
	BDW	58.3	19.3	1.4
	BL	58.8	21.2	2.3
$^{16}N, 2^-$	CGLN	471	19.2	2.1
	BDW	472	15.7	1.7
	BL	476	17.3	2.4
$^{12}B, 2^+$	CGLN	327	304	19.9
	BDW	360	322	15.9
	BL	391	393	23.7
$^{16}N, 1^-$	CGLN	22	156	17.6
	BDW	24	158	13.7
	BL	25	188	20.8
$^{16}N, 3^-$	CGLN	304	352	26.8
	BDW	327	358	20.9
	BL	348	416	31.2

due to spin-dependent and spin-independent parts of the amplitude. Table 2 illustrates the effect quantitatively. We conclude that at low pion energies the nuclear transitions can, in principle, be used as a selector of elementary amplitudes. This point is discussed in ref./12/.

4.7. Along with the pion photoproduction reaction the inverse process - the radiative in-flight pion capture seems to be of interest, too. The first experimental results have already been published. Some advantage of the in-flight capture as compared with the photoproduction can be traced to the beam quality. In the photoproduction reaction up to now the bremsstrahlung photons (continuous spectrum) are used. In the case of the pion electroproduction one should know the virtual photon spectrum. The in-flight capture is free of these problems. The intensity of pion beems, however, even at modern mesonic factories is still too low to have a reaction yield allowing wide applications.
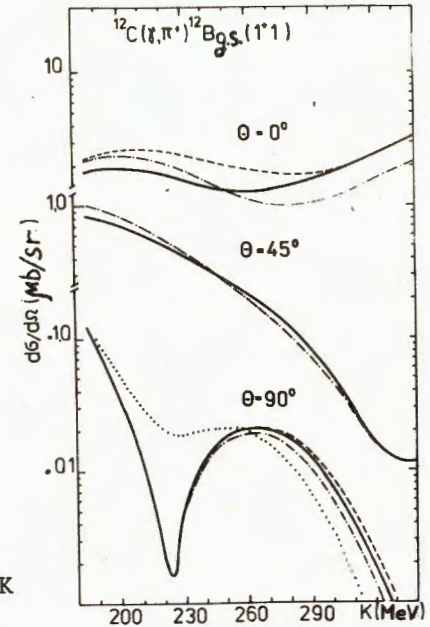

Fig.11. Pion photoproduction in ^{12}C with 1^+ level excitation (see fig.2). The solid line - DH wave function, the dotted line - CK wave function and CGLN-amplitude.

5. CONCLUSION

We have considered three ingredients of the problem of pion photoproduction on complex nuclei. One of the main results obtained points to the strong dependence of pion photoproduction cross sections on the nuclear structure input. Before starting the analysis of the (γ, π) or (π, π') reactions one should have an exhaustive information on the nuclear matrix elements. Their ambiguity in several recent calculations is such that they may cause a deviation by an order of magnitude in the pionic cross sections. When extracting the nuclear matrix elements from electron scattering data a correct analysis of the electric-type form factors should include the continuity equation.

The developed on-shell version of DWIA for pion photoproduction seems to be attractive due to its simplicity. The results obtained indicate that this method works satisfactorily. One can use it for a systematic analysis of the basic features of the pion photoproduction on light nuclei.

REFERENCES

1. Laget J.M. Phys.Rep., 1981, v. 69, p.1.
2. Laget J.M. Lecture Notes in Physics, 1981, v. 137, p. 148. Springer-Verlag, B.-H.-N.Y.
3. Singham M.K., Tabakin F. Ann.Phys., 1981, v. 135, p. 71.
4. Bernstein A.M. In: Int.Energy Nucl.Phys. (Eds. R.Berger, S.Costa, C.Schaerf). World Scientific, Singapore, 1982, p. 125.
5. Gmitro M., Mach R. Zeit.Phys., 1979, v. A290, p. 179. Gmitro M., Kvasil J., Mach R. Phys.Lett., 1982, v. 113B, p. 205. Gmitro M. et al. JINR, P4-83-403, Dubna, 1983.
6. Eramzhyan R.A. et al. J.Phys.G: Nucl.Phys., 1983, v.9, p. 605.
7. Eisenberg J. Nucl.Phys., 1982, v. A389, p. 595.
8. Lenz F., Thies M., Horikawa Y. Ann.Phys., 1982, v. 140, p. 266.
9. Chew G.F. et al. Phys.Rev., 1957, v. 106, p. 1345.
10. Berends F.A. et al. Nucl.Phys., 1967, v. B4, p.1.
11. Blomqvist I., Laget J.M. Nucl.Phys., 1977, v. A280, p. 405.
12. Kamalov S.S., Kaipov T.D. JINR, P4-83-539, Dubna, 1983.
13. Cohen S., Kurath D. Nucl.Phys., 1965, v. 73, p.1.
14. Graves R.D. et al. Can J.Phys., 1980, v. 58, p. 48.
15. Dubach J., Haxton W.C. Phys.Rev.Lett., 1978, v. 41, p.1453.
16. Richter A. Nucl.Phys., 1982, v. A374, p. 177.
17. Donnelly T.W., Walecka J.D. Phys.Lett., 1972, v.B41, p.275.
18. Ansaldo E. et al. Nucl.Phys., 1979, v. A322, p. 237.
19. Heisenberg J., Blok H.P. Ann.Rev.Nucl.Sciences 1983, v. 33. p. 2224.
20. Eramzhyan R.A. et al. JINR, E4-83-543, Dubna, 1983.
21. Friebel A. et al. Nucl.Phys., 1978, v. 294, p. 129.
22. Eramzhyan R.A. et al. Phys.Lett., 1983, v. 128B, p. 371; JINR, E4-83-296, Dubna, 1983.
23. De Carlo V., Freed N. Phys.Rev., 1982, C25, p. 2162.
24. Eramzhyan R.A. et al. JINR, E4-83-574, Dubna, 1983.
25. Gmitro M. et al. Sov. J. Particles and Nuclei 1982, v. 13, p. 1230; 1983, v. 14, p. 879.
26. Jennewein P., Schoch B., Zettl F. Preprint, Mainz, 1983.

Эрамжян Р.А. и др.   E4-84-67
Фоторождение и радиационный захват пи-мезонов на ядрах

Анализируются парциальные переходы в реакции фоторождения и радиационного захвата пи-мезонов на примере ядер $^{10}B, ^{12}C, ^{16}O$ совместно с реакциями неупругого рассеяния электронов и пи-мезонов. Обсуждается зависимость характеристик переходов от ядерных матричных элементов, амплитуды фоторождения на нуклоне и характера пион-мезонного взаимодействия. Показана необходимость использования уравнения непрерывности в процессе неупругого рассеяния электронов. В рамках "on-shell" варианта DWIA получено удовлетворительное согласие с имеющимися экспериментальными данными.

Eramzhyan R.A. et al.   E4-84-67
Pion Photoproduction and Radiative Pion Capture on Nuclei

Partial transitions in pion photoproduction and radiative pion capture on 1p-shell nuclei are analysed together with the electron and pion scattering. The $^{10}B, ^{12}C$, and ^{16}O nuclei are considered as examples. The dependence of the transition characteristics on nuclear matrix elements, photoproduction amplitude, and pion-nucleus interaction is discussed.